An Improved Topology Graph and Ant Colony Optimization Approach for Optimizing Electric Vehicle Travel Path Considering Time and Charging Cost

Liang Wei*
School of Automotive Engineering and General Aviation, Shaanxi Vocational & Technical College Xi'an 710038, China
E-mail: wei_liang1986@163.com

Keywords: electric vehicles, ant algorithm, topology graph, time, cost

Received: July 15, 2024

The integration of high-tech in electric vehicles enhances the driving experience, which is more environmentally friendly. However, the uneven distribution of charging stations and limited battery capacity require a balance between travel time and charging cost during long-distance travel. Different charging strategies and path planning can lead to different charging cost and travel time. Introducing artificial intelligence into path planning aims to enhance the long-distance travel experience for drivers and passengers. Therefore, the study adopts topology graphs to isomerize the roads during travel, and the algorithm topology graph is improved to remove redundant paths. Then, it is combined with ant algorithm to construct a path optimization model. The experiment used the electricity price in C1 city and the charging charging parameters in the parking lot at Ya as experimental data to simulate the real environment. The simulation results showed that the research algorithm achieved convergence after the 23rd iteration, with a comprehensive total cost of 38. The computational efficiency and results are superior to other algorithms. The average total cost of the travel path optimization model based on improved topology and ant algorithm was 7% -26% lower than other models. The results indicate that the research model has a better balance effect when considering travel time and charging cost comprehensively, which can plan the optimal travel strategy. The research results can make a positive contribution to autonomous driving.

Povzetek: Predlagan je izboljšan pristop optimizacije poti električnih vozil, ki združuje topološke grafe in algoritem kolonije mravelj, znižuje skupne stroške potovanja ter uravnoteži čas in stroške polnjenja.

1 Introduction

With the rapid development of battery energy storage technology and intelligent interaction between humans and vehicles, electric vehicles have environmental protection, intelligence, diverse choices, and high cost-effectiveness. More people choose to purchase electric vehicles [1-2]. However, in long-distance travel, the distribution of charging stations is not as wide as that of gas stations, and electric vehicles have a shorter range than gasoline vehicles. Frequent visits to charging stations for energy storage make it difficult for drivers to balance the time and charging cost of long-distance travel [3]. Due to different congestion situations during visits to charging stations, there are differences in tiered electricity prices, resulting in varying levels of electricity when arriving and leaving the stations. This greatly increases the difficulty of planning the optimal travel plan. Therefore, finding an electric vehicle path optimization method that comprehensively considers time and charging cost can greatly enhance the driver's long-distance travel experience. However, Algorithm Topology Graph (ATG) can isomerize complex road networks and charging stations into point and edge sets during travel, with clear connectivity and sequential relationships, which can simplify complex path problems [4-5]. Ant Colony Optimization (ACO) algorithm simulates ant foraging and has a global self-organizing search and positive feedback mechanism. After iteration, it gradually obtains the global optimal solution from the local optimal solution, which is suitable for travel path optimization [6-8]. Many scholars and experts have conducted relevant research on ATG and ACO. Details are shown in Table 1.

Table 1: The summary table of the reviewed research

Reference	Method	Result	Inadequacy
Dawen [9]	Based on bidirectional heuristic search A-star and ACO algorithm	Compared with the heuristic search A-star algorithm, acyclic algorithm, and Gurobi algorithm, it reduces 102.73m, 73.27m and 23.08m, respectively	ACO algorithm can fall into local optimal solution, and its robustness and generalization ability have not been explored
Dong et al [10]	Multi-objective ACO for ship pipeline path design method	The actual ship pipeline path design and simulation experiments show that this method improves the efficiency of the design work	ACO has strong optimization ability, and it needs to be verified for path planning
Zhao et al [11]	A multi-material, multi-volume topology optimization framework	Compared with the conventional frame, the optimized frame has a 17.4% reduction in steel content and fewer cracks under the ultimate load	The topology of steel structure is deterministic, while the topology of the path planning is multivariate and uncertain
Kai et al [12]	Elastoplastic continuum topology optimization method based on SIMP framework	The stable load bearing capacity of the elastoplastic continuum is increased by 6.1%	This study uses SIMP framework to optimize the topology structure, which is not suitable for the content of the study

To solve the traffic congestion and increased fuel consumption caused by blind navigation during travel, Xia et al. proposed a bidirectional heuristic search algorithm based on A-star and ACO. The research results indicated that the length of the shortest path recommended by this algorithm was 102.73m, 73.27m, and 23.08m shorter than heuristic search A-star algorithm, acyclic algorithm, and Gurobi algorithm, respectively [9]. Dong et al. proposed a multi-objective ACO-based ship pipeline path design method, which addressed the extremely complex nature of ship pipelines and the high workload and low design efficiency involved in designing ship pipeline paths. The study conducted simulation experiments and applied this method to the ship pipeline path design in reality. The feasibility and effectiveness of this method were verified through simulation experiments and practical use, which improved the efficiency of design work [10]. Zhao et al. designed a multi material and multi volume topology optimization framework to address the cost increase caused by the need for a large number of crack control steel bars in deep beam design. Compared with traditional frameworks, the optimized framework reduced steel content by 17.4% and had fewer cracks under ultimate load. The topology structure can reduce the steel cost in deep beam design [11]. Li and Cheng proposed a topology optimization method for elastic-plastic continuum based on SIMP framework to address the low stability load bearing performance of elastic-plastic continuum. The experimental results showed that the stability load bearing capacity of the elastic-plastic continuum was improved by 6.1%. From this, the topology optimization of elastic-plastic continuum can effectively improve performance [12].

The above research indicates that some scholars have conducted relevant research on ATG and ACO, which are helpful for path planning and cost control. However, there is very little research on the combination of ATG and ACO for electric vehicle path planning. Therefore, this study combines ATG and ACO to the travel path optimization, constructing an optimal long-distance travel path selection model that can balance travel time and charging cost. It is expected that this model can take into account different drivers' perceptions of time and cost, fully consider all traffic related time and toll cost during travel, and select the optimal travel path to improve the driver's driving experience. The innovation of this study lies in the proposed model, which combines the roads, starting points, endpoints, and charging stations in long-distance travel into a topology graph. The topology graph is iteratively optimized using the ATG-ACO algorithm to calculate the optimal path for comprehensive time and cost. The contribution of the research lies in not only being able to calculate the global optimal solution for long-distance travel, but also automatically balancing charging cost and overall travel time based on different user preferences through conversion and weighting coefficients. At the same time, the proposed optimization strategy for electric vehicle travel routes has broad application prospects and promotion value, which is expected to make positive contributions to the development of industries such as autonomous driving and logistics distribution.

The research is mainly divided into five parts. The first part is the introduction, which analyzes the research results of long-distance travel solutions and briefly describes the optimization strategies proposed in the study. The second part designs a travel path planning model based on the ATG-ACO algorithm. The third part is model simulation testing. The fourth part discusses the simulation test results. The fifth part summarizes the research results. The path optimization model based on ATG and ACO can calculate the optimal travel strategy that comprehensively considers travel time and charging cost.

2 Methods and materials

Topology graphs can isomerize the positions and paths during travel in the form of point and edge sets, better representing dependency relationships and execution order, making it easier for algorithms to find the optimal path [13-14]. This study improves the topology algorithm and decomposes the total cost of travel time and charging cost to establish a cost calculation method that considers conversion coefficients, weighted coefficients, and mutual constraints between sub-items. The ant algorithm is introduced into the preprocessed topology to form a travel path planning model based on the ATG-ACO algorithm. Through algorithm iteration, the global optimal solution is gradually obtained from the local optimal solution, which comprehensively considers the time and charging cost of the optimal path.

2.1 Design of improved ATG algorithm based on electric vehicle travel path

Electric vehicles have fewer charging stations than gas stations, which greatly increases the difficulty of path optimization due to frequent charging, queuing for charging, and tiered electricity prices. An improved ATG that heterogeneous travel locations is proposed, characterized by clear hierarchical structure, acyclic and traversal characteristics. These advantages facilitate the modeling of travel paths, allowing algorithms to efficiently find the optimal path from a large number of calculations. Considering the objective relationship between remaining electricity, storage capacity, and charging time, when constructing a topology diagram, the following constraints must be met. Firstly, the uni-directionality of the battery electrochemical conversion process makes it impossible to charge and discharge simultaneously. Therefore, there is a mutually exclusive constraint, as shown in equation (1).

$$\eta + \gamma \le 1 \tag{1}$$

In equation (1), η represents the charging state of the vehicle, and $\eta = \{0,1\}$. $\eta = 0$, indicates that the vehicle is not charging. $\eta = 1$, it indicates that the vehicle is currently charging. γ is the discharge state of the vehicle, and $\gamma = \{0,1\}$. When $\gamma = 0$, the vehicle is not discharging. When $\gamma = 1$, the vehicle is discharging. In addition, the constraint of battery capacity should be considered. Firstly, when reaching the charging station, the amount of electricity must be greater than or equal to 0. Secondly, the amount of energy stored cannot exceed the battery capacity E_M. The constraint of remaining battery capacity E_x is shown in equation (2).

$$E_x = \begin{cases} E_x \ge 0 \\ E_x + Q_x \chi T_x \le E_M \end{cases} \tag{2}$$

In equation (2), Q_x is the charging power of the charging station. χ is the charging efficiency of the vehicle. T_x is the charging time at charging station x. Finally, because there is a relationship between the locations, it is necessary to consider the time constraint of reaching the charging station. The expression for the arrival time constraint is shown in equation (3).

$$T_b = \begin{cases} T_s + \dfrac{D_{ab}}{\overline{V}_{iab}} & \left(a \in 0, b \in B_a or \left(\Lambda \cap a\right)\right) \\ T_a + \dfrac{D_{ab}}{\overline{V}_{iab}} & \left(a \in \Phi, b \in B_a or \left(\Lambda \cap a\right)\right) \\ T_a + T_{Wb} + T_{Cb} + \dfrac{D_{ab}}{\overline{V}_{iab}} & \left(a \in \Lambda, b \in B_a\right) \end{cases} \tag{3}$$

In equation (3), T_b is the time to reach charging station b. D_{ab} is the distance between charging station a and b. $\overline{V}_{iab}$ is the estimated average speed of the section. T_s is the starting time. T_a is the time to leave a. T_{Wb} is the waiting time for the vehicle to be charged in queue at b. T_{Cb} is the charging time of the vehicle at b. The set of rechargeable locations around a is B_a. Λ is the collection of charging stations where the car undergoes charging. Φ is the collection of all charging stations for charging during travel, including fast charging stations and regular parking lots with charging stations. Taking into account the above constraints, the topology diagram presents an extremely complex structure that requires a significant amount of computational time. Therefore, the ATG is optimized to improve computational efficiency. The traditional simplified topology and the improved ATG are shown in Figure 1.

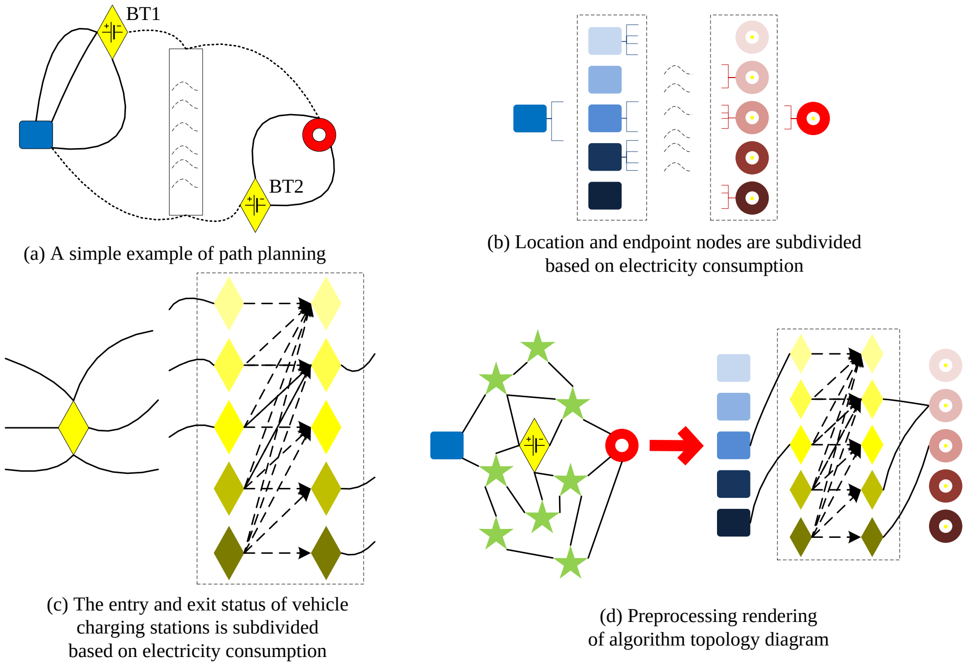

Figure 1: Newly constructed algorithm topology graph

Figure 1 (a) shows a simplified topology structure. In Figure 1 (b), based on the remaining power of the vehicles at the starting and ending points, the study divides the starting and ending points into 5 new nodes using a 20% gradient. In Figure 1 (c), the charging station is divided into 10 new nodes based on the remaining battery capacity of the vehicle after leaving the charging point and arriving at the next charging point, using a 20% gradient. The edge formed between two charging points increases from one edge to 15 edges. The study proposes an improved algorithm for preprocessing the topology graph, aiming to evaluate whether to add new edges and remove edges connecting two long-distance charging stations to construct a sparser topology. As shown in Figure 1 (d), an improved topology is obtained by removing these two redundant edges. The specific preprocessing algorithm flow is shown in Figure 2.

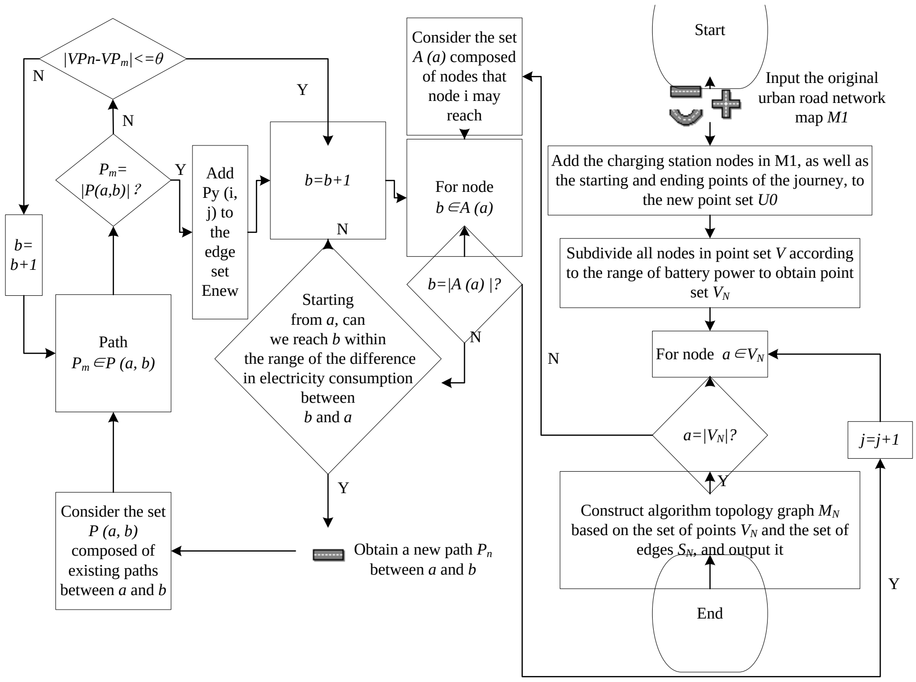

Figure 2: Preprocessing process of algorithm topology graph

In Figure 2, the starting point, ending point, and road network in travel are first heterogeneous into point set $U0$. Based on the above partitioning strategy, a new point set U_N is obtained. Then, whether a is within the U_N is determined. If so, the ATG M_N is constructed based on the point set U_N and edge set S_N. If not, a and b form a new edge P_n from newly generated nodes. If the absolute value of the difference in the comprehensive cost of all existing paths P_m between P_n and a, and b is greater than the threshold P_n, it indicates that the new path P_n can be added to the edge set. The original path will be removed as a redundant path. Through the above algorithm process, topology optimization and simplification are achieved, significantly improving the efficiency and performance of the topology structure.

2.2 Comprehensive cost calculation method for balancing time and charging cost

The improved ATG simplifies complex path planning problems. To find the optimal comprehensive cost solution that balances travel time and charging cost from the improved topology graph, mathematical modeling is performed on the comprehensive cost. The modeling approach is to break down the total cost and calculate it separately. The schematic diagram of total cost division is shown in Figure 3.

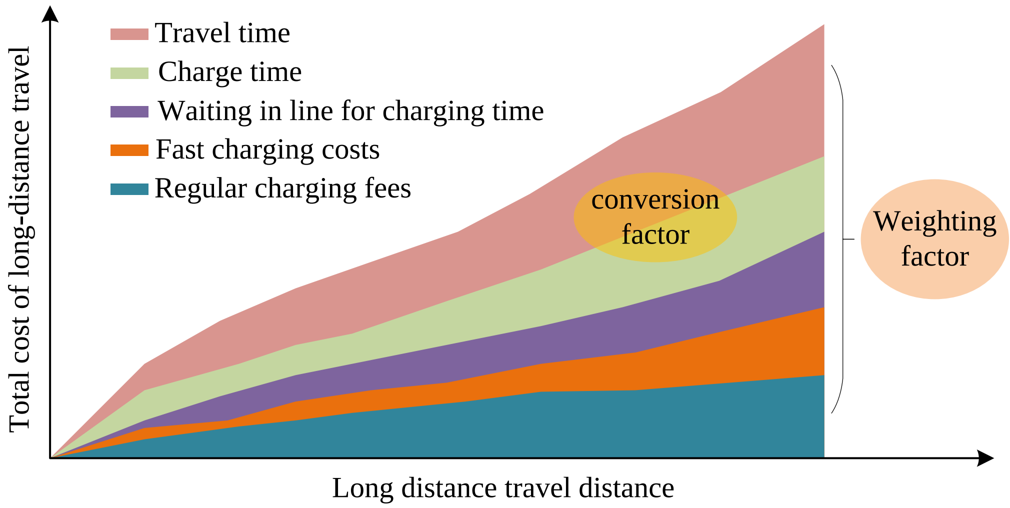

Figure 3: The comprehensive cost of electric vehicle travel

In Figure 3, starting from the starting point, the five types of costs continue to increase as the travel distance increases. Different drivers have different understandings of the value of time and have different requirements for the overall budget. Therefore, different weighting coefficients are set for different drivers regarding driving time, charging time, waiting time for charging, fast charging fees, and regular charging fees. In addition, conversion factors are set for travel time, charging time, and waiting time for charging, converting time into expenses and simplifying the calculation of target cost. Therefore, the comprehensive minimum cost is shown in equation (4).

$$min(A_{all}) = min(\alpha \times \beta T_{all} + (1-\alpha) C_{all}) \quad (4)$$

In equation (4), A_{all} represents the total comprehensive cost. α is the weighting coefficient. β is the conversion factor. T_{all} is the sum of three time sub items. C_{all} represents the total charging cost. Firstly, the total driving time T_d is calculated, as shown in equation (5).

$$T_d = \sum_{a \in U_a} \frac{l_{ai}}{v_{ai}} + \eta_{ai} \times \lambda_{ai} \times \varepsilon_{ai} \quad (5)$$

In equation (5), the road section that the car passes through is set U_a. l_{ai} is the length of road section ai. v_{ai} is the average speed of the road segment calculated based on traffic data. η_{ai} is the set $\{0,1\}$. 1 represents the presence of traffic lights on the road section ai, and 0 represents the absence of traffic lights on the road section ai. λ_{ai} is the probability of a car encountering a red light on section ai. ε_{ai} is the time when cars wait for red lights on the section ai. Then, the total waiting time for charging is calculated. To calculate the waiting time for charging, whether all charging stations are occupied should be considered. The probability P_{ant} of all charging stations being occupied is calculated using equation (6).

$$P_{ant} = \begin{cases} \dfrac{(\frac{\varphi_{at}}{\mu_{a,t}})^n}{n!} P_{a0t} & n = 1,2,3,4,5,...,W_a \\ \dfrac{(\frac{\varphi_{at}}{\mu_{a,t}})^n}{W_a!\ W_a^{\,n-W_a}} P_{a0t} & n > W_a \end{cases} \tag{6}$$

In equation (6), φ_{at} is the car arrival rate. $\mu_{a,t}$ is the parameter charging rate. W_a is the total number of charging stations. P_{a0t} represents the probability that all charging stations are not used within t. The P_{a0t} is shown in equation (7).

$$P_{a0t} = [\sum_{i=0}^{W_a-1} \frac{(\frac{\varphi_{j,t}}{\mu_{j,t}})^i}{i!} + \frac{(\frac{\varphi_{j,t}}{\mu_{j,t}})^{W_a}}{W_a!(1-\frac{\varphi_{j,t}}{W_a \mu_{j,t}})}]^{-1} \tag{7}$$

In equation (7), i is the count of charging stations in a charging station. According to equation (6), the average queue length S_{at} of charging station a within time slot t is shown in equation (8).

$$S_{at} = \sum_{n=W_a+1}^{\infty} (n-W_a) \times P_{ant} = \frac{(\frac{\varphi_{j,t}}{\mu_{j,t}})^{W_a} \times \frac{\varphi_{j,t}}{W_a \mu_{j,t}}}{W_a!(1-\frac{\varphi_{j,t}}{W_a \mu_{j,t}})^2} \times P_{a0t} \tag{8}$$

According to queue probability, length, etc., the total waiting time for charging in the queue is shown in equation (9).

$$T_W = \sum_{a \in B_a} T_a^{\,w} = \sum_{a \in Ba} \frac{S_{at}}{\varphi_a} \tag{9}$$

Afterwards, the total charging time T_C is shown in equation (10).

$$T_C = \sum_{a \in B_a} T_a^{\,C} = \sum_{a \in Ba} \frac{E_a}{Q_a \chi} = \sum_{a \in Ba} \frac{E_a^{\,live} - E_a^{\,arrive}}{Q_a \chi} \tag{10}$$

In equation (10), $E_a^{\,live}$ is the amount of electricity that the car leaves a. $E_a^{\,arrive}$ is the amount of electricity that the car reaches a. E_a is the amount of electricity stored. Q_a is the power of the a charging station. After obtaining the three-time costs, the charging fees are calculated separately. The regular charging fee is equal to the cost in a regular parking lot. The study considers that cars discharge electricity in the parking lot to obtain partial income from the power grid. Therefore, the detailed composition of the total cost breakdown is shown in Figure 4. As shown in Figure 4, driving time consists of driving time and waiting time at red lights, while the slow charging fee is the difference between the charging fee and the discharge income. The fast-charging fee C_f is shown in equation (11).

$$C_f = Q_f \sum_{a \in Ba} \sum_{t=t_a+T_a^W}^{t=t_a+T_a^W+T_a^C} \times \partial_t \times \Delta T \tag{11}$$

In equation (10), t_a is the time to reach the a charging station. ΔT is the time spent on decision-making. Q_f is the fast charging power. ∂_t is a tiered electricity price. The ordinary charging fee C_S is shown in equation (12).

$$C_S = Q_s \sum_{t=T_e}^{T_{ns}} \partial_t \eta \Delta T - Q_{dis} \sum_{t=T_e}^{T_{ns}} \gamma_t \eta_t \Delta T \tag{12}$$

In equation (12), γ_t represents the purchase price of electricity from the power grid. T_e is the end time of this trip. T_{ns} is the start time of the next trip. Q_{dis} is the discharge power. Q_s is the slow charging power.

2.3 Construction of comprehensive cost travel path planning model based on ATG-ACO

The preprocessed ATG is introduced into the path optimization algorithm to obtain the optimal path for electric vehicle travel. Considering that the preprocessing process of ATG includes judgment and feedback mechanisms, and finding the optimal path from a topology with numerous elements is a highly complex problem, the study introduces ACO. The ACO algorithm has the characteristics of positive feedback, self-organization, and global search, making it very suitable for complex path planning [15]. The principle of ACO is shown in Figure 5.

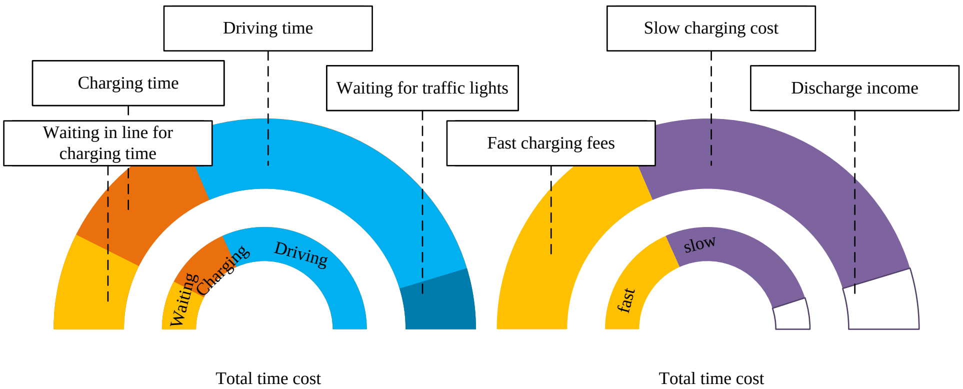

Figure 4: Detailed composition of total cost

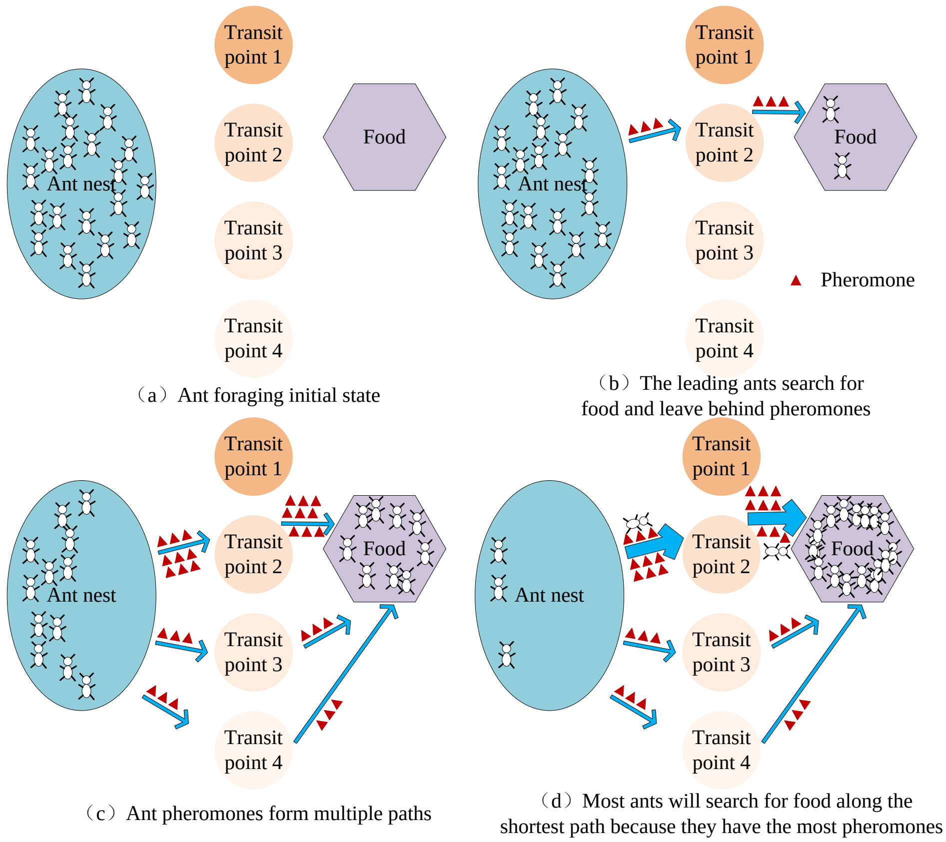

Figure 5: Ant algorithm schematic diagram

Figure 5 (a) shows the initial state of ants foraging, with four passing points in the ant nest away from food. In Figure 5 (b), the leading ant passes through point 2 to reach the food, leaving behind pheromones between them. In Figure 5 (c), a large number of ants reach the food, leaving behind pheromones that form multiple paths. In Figure 5 (d), Path 2 leaves the most pheromones, and most ants will search for food along this shortest path. Ants leave more pheromones on the path of the optimal solution through the action of pheromones, attracting ants to choose this path and guiding the ant colony to the optimal path. The path finding process of applying ACO to ATG is as follows. Firstly, the initialization parameters include the number of ants A_s, the total amount of released pheromones, volatility factor ϑ, importance factor π, the importance factor ψ of the heuristic function, the number of iterations δ, and the concentration of pheromones ω. If charging station b is adjacent to charging station a, then the edge ω_{ab} between a and b is 1. If not adjacent, then ω_{ab} is 0. Ants start from the starting point and reach the next node according to probability p_{ab}^{δ}. The probability calculation for ants from node a to node a is shown in equation (13).

$$p_{ab}^{\delta} = \begin{cases} \dfrac{[\omega_{ab}]^{\vartheta}[\Delta]^{\pi}}{\sum_{b\in B_a}[\omega_{ab}]^{\vartheta}[\Delta]^{\pi}}, & b \in B_a \\ 0, & b \notin B_a \end{cases} \tag{13}$$

In equation (13), Δ is the heuristic function [16]. When all ants in the δ-th iteration stop searching, the time and charging cost of the electric vehicle represented by all ants to the endpoint are calculated, and obtain the local optimal solution for the δ-th iteration. The path decision variable x_{ab} is updated based on the arrival of ants at the node. The decision variable is shown in equation (14).

$$x_{ab} = \begin{cases} 1, & b \ \ is \ \ selected \\ 0, & b \ \ isn't \ \ selected \end{cases} \tag{14}$$

In equation (14), when $x_{ab}=1$, the vehicle's battery level represented by the ant is updated. The battery level update calculation is shown in equation (15).

$$q_{ant}' = q_{ant} - \sum_{b\in allowed_{a,ant}} x_{ab} \times Dis(x_{ab}) \times \overline{E}_1 \tag{15}$$

In equation (15), q_{ant}' is the updated electricity level. $\overline{E}_1$ and $Dis(x_{ab})$ represent the power consumption per unit distance and the distance of a and b, respectively. If the ant fails to find the global optimal solution, it updates the pheromone for the next iteration and triggers a positive feedback mechanism. The pheromone updating is shown in equation (16).

$$\omega_{\delta+1} = (1-\vartheta)\omega_{\delta} + \sum_{R=1}^{R} \Delta\delta^{R} \tag{16}$$

In equation (16), $\omega_{\delta+1}$ represents the concentration of pheromones after the next iteration. R is the number of ants that reach the endpoint after $\delta+1$ iterations. $\Delta\delta^R$ is the pheromone increment [17]. The pheromone increment is shown in equation (17).

$$\Delta\delta^{R} = \frac{\square}{A_{T,C}^{R}} \tag{17}$$

In equation (17), $A_{T,C}^{R}$ is the distance to the destination. The calculation method for determining whether to continue iteration is shown in equation (18).

$$\delta_{next} = \delta_n + 1 < \delta_{max} \tag{18}$$

The above steps are repeated to the maximum number of iterations δ_{max}. The ants search for the global optimal solution. The above process uses ant simulation to find the optimal path for electric vehicles. The process of searching for the optimal comprehensive cost in the preprocessed topology is shown in Figure 6.

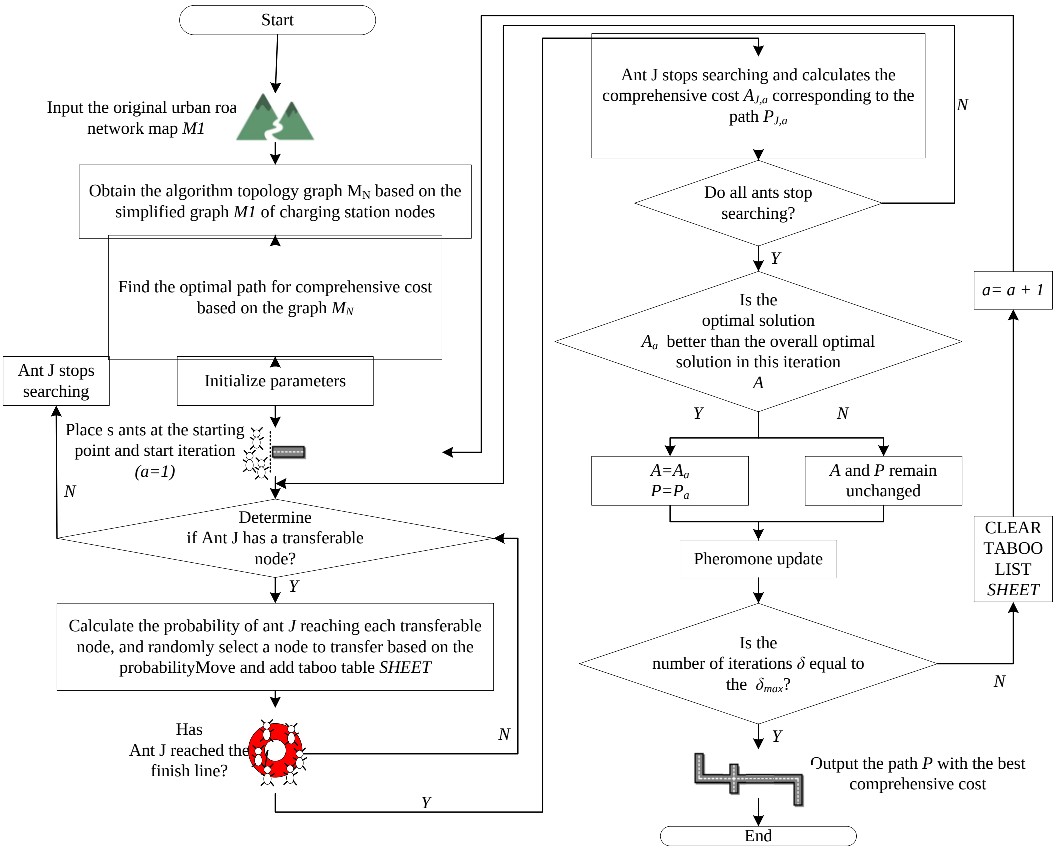

Figure 6: A Topology preprocessing ant colony path optimization algorithm framework

As shown in Figure 6, the road network diagram $M1$ is first heterogeneous into an improved ATG M_N. Then, ants simulate the travel scenario of electric vehicles, randomly select charging nodes from the starting point on the journey, and optimize the selected path through iteration. Finally, the most cost-effective travel route is determined.

3 Results

The travel path planning model based on ATG-ACO algorithm is simulated and tested. A simulation environment using road network $M1$ is established, and relevant parameters are set.

The improved ATG-ACO algorithm is iteratively trained to test the convergence efficiency of the algorithm. The ACO is compared with ATG-ACO algorithm to analyze the effect of the ATG on improving computational efficiency. Finally, a comparative experiment is conducted between the designed model and other models to verify that the proposed model can find the optimal path considering time and charging cost.

3.1 Simulation environment and parameter settings

To simulate a real environment, the electricity step tariff in C1 city and the charging station parameters in the parking lot at Ya are selected as experimental data. The detailed information of the sample is shown in Table 2.

Table 2: Data samples selected from the case western storage bearing dataset

Electric vehicle parameters		Charging station parameters		Parking lot parameters		Time-of-use			
Parameter	Value	Parameter	Value	Parameter	Value		Peak period	Ordinary segment	Low valley section
Unit energy consumption (kWh/km)	0.15	Charging power	90	Charging power (kW)	20	Period of time	7:00-11:00	23:00-7:00 the next day	11:00-19:00
	22.6	Charge efficiency	80%	Discharge power (kW)	20		19:00-23:00		
Battery capacity (kWh)	/	Profit coefficient	Random numbers between [1,1.5]	Charge efficiency	80%	Charging price	1.3155	0.0.8399	0.3822
/	/	/	/	Discharge efficiency	80%	Electricity purchase price	/	0.8399	/

The study selects ACO without ATG as the comparison object with path planning models based on DPO, QLPO, and PGAPO proposed by another research.

3.2 Analysis of iterative convergence and computational efficiency of ATG-ACO

After constructing a simulation experimental environment, the ATG-ACO algorithm is iteratively trained and compared with other algorithms. The experimental results are shown in Figure 7. In Figure 7, the research algorithm converged after 23 iterations, and the calculated optimal cost was 38. The QLPO algorithm converged after 74 iterations, and the optimal cost was 49. The convergence speed of PGAPO algorithm and DPO algorithm was relatively slow. PGAPO converged after 90 iterations, with an optimal cost of 73. The DPO algorithm fluctuated up and down as the number of iterations increased, and still did not converge after 120 iterations. From this, the proposed ATG-ACO has better convergence speed than other algorithms, and the optimal planning cost is the lowest. To analyze the improvement effect of improved topology in ATG-ACO, a comparative experiment is conducted between ACO and ATG-ACO. The results are shown in Figure 8.

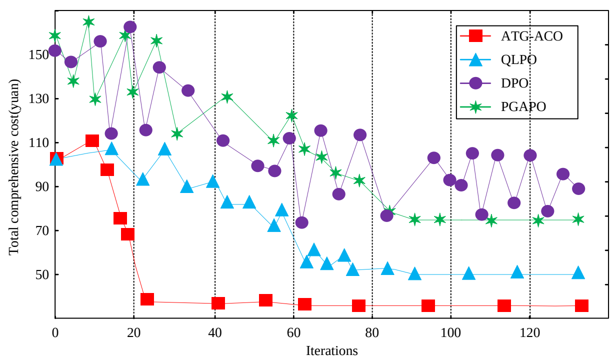

Figure 7: Comparison chart of algorithm iteration training convergence

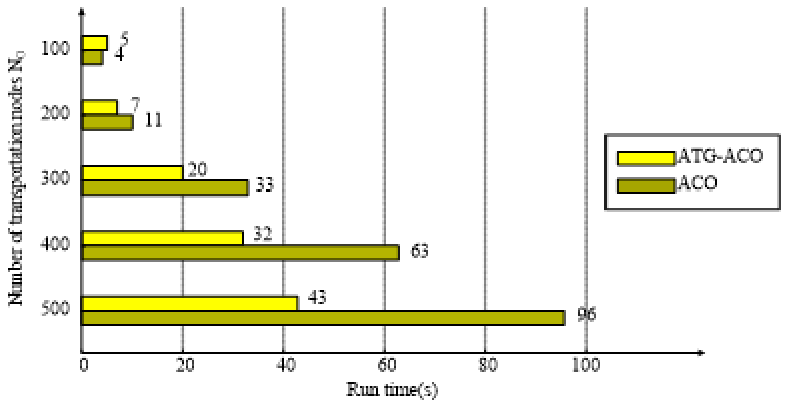

Figure 8: Comparative experimental results of ATG and ATG-ACO

In Figure 8, with 100 traffic points, the ATG-ACO algorithm took 1s longer than the ACO algorithm. As the number of traffic points increased, the ATG-ACO algorithm took less time than the ACO algorithm. The differences were more pronounced when there were multiple traffic points. When the number of traffic points was 300, the ATG-ACO algorithm took 20s, while the ACO algorithm took 33s. When the number of transportation nodes was 500, the ATG-ACO algorithm took only 43s, less than half of the time of the ACO algorithm. The results indicate that topology preprocessing has a great promoting effect on ant algorithm in finding the optimal solution.

3.3 Comprehensive cost control analysis of travel path planning model based on ATG-ACO algorithm

The above experiment shows that the ATG-ACO algorithm has better computational efficiency. The study compares the ATG-ACO path planning model with other models mentioned above. The charging cost results after multiple simulation experiments are averaged, as shown in Figure 9. In Figure 9, as the weighting coefficient of travel time increased from 0 to 1, the total charging cost of the optimal path planned by the ATG-ACO model gradually increased from 35 to 48 yuan. When the weight coefficient of the QLPO model was 0.25, the charging cost decreased to the lowest value of 29 yuan, and increased to 37 yuan as the weight value increased. From Figure 9, the DPO model is most affected by the weighting coefficient, with the largest increase, and the total charging cost increases from 35 yuan to 67 yuan. However, the QLPO model is least affected by weighting coefficients, and the charging cost remains around 47 yuan. From this, the weighting coefficient, when only considering the total charging cost during long-distance travel for path optimization planning, is not entirely superior to other path planning models, because the designed model not only considers charging cost but also balances the time cost of travel. The total travel time after multiple simulation experiments to obtain the average value is shown in Figure 10.

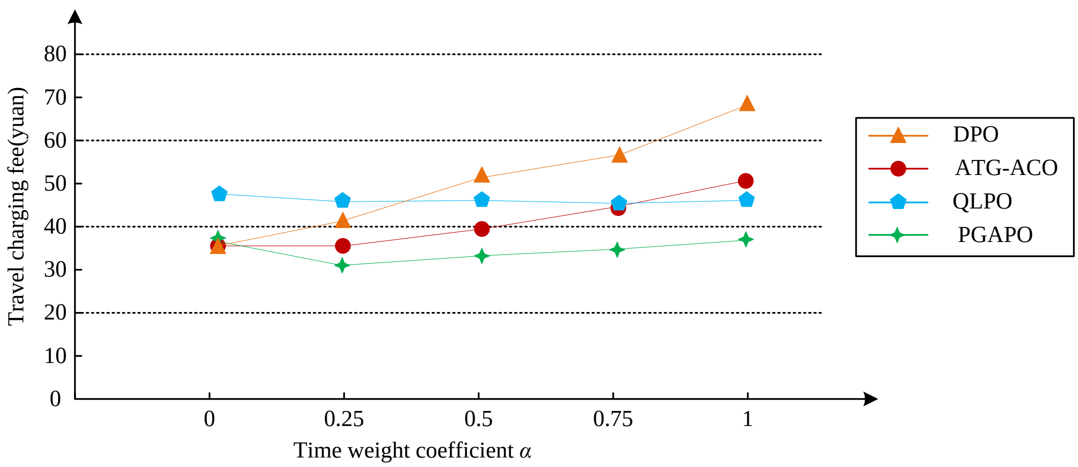

Figure 9: Nightingale diagram of three experimental results

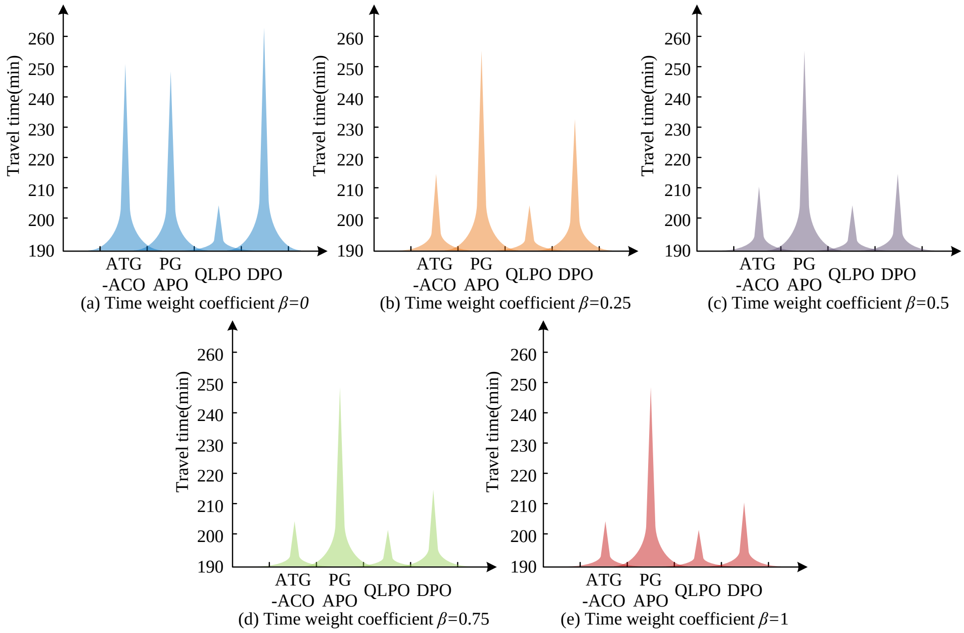

Figure 10: The total travel time results of various model comparison experiment

In Figure 10 (a), the total time of the ATG-ACO model was 252s, which was better than the total time 264s of the DPO, but 59s more than the QLPO. The total time of the ATG-ACO model in Figure 10 (b) was 213s, which was also better than the PGAPO and DPO models, but 10s longer than the QLPO. The total optimal path time of the ATG-ACO model in Figures 10 (c), 10 (d), and 10 (d) were 209s, 204s, and 203s, respectively, which were close to the QLPO and significantly lower than the PGAPO and DPO models. From this, when only considering the single time cost, ATG-ACO is not entirely superior to other models. The study converts the total time into the total charging cost through a conversion coefficient. The experimental results considering the total comprehensive cost are shown in Figure 11. From Figure 11 (a), due to the conversion coefficient, the lowest comprehensive cost of the ATG-ACO model was 78 yuan, and the highest value was 88 yuan. Regardless of the weighting coefficient, it is superior to other models. The proposed ATG-ACO model is the optimal model for path planning, taking into account the balance between travel time and charging cost.

4 Discussion

This study compares the performance of the ATG-ACO and analyzes the comprehensive cost control effect of the travel path planning model based on the ATG-ACO algorithm. The results showed that the ATG-ACO algorithm exhibited significant advantages in convergence speed and computational efficiency in optimal path planning. In the comparison of convergence curves, the ATG-ACO algorithm completed convergence after the 23rd iteration, with a total cost of 38 lower than other algorithms. This result is similar to the results obtained by Abdullah et al. in their study combining improved ATG and ACO [18]. This result indicates that the ATG-ACO algorithm can quickly find the optimal solution, and improve the

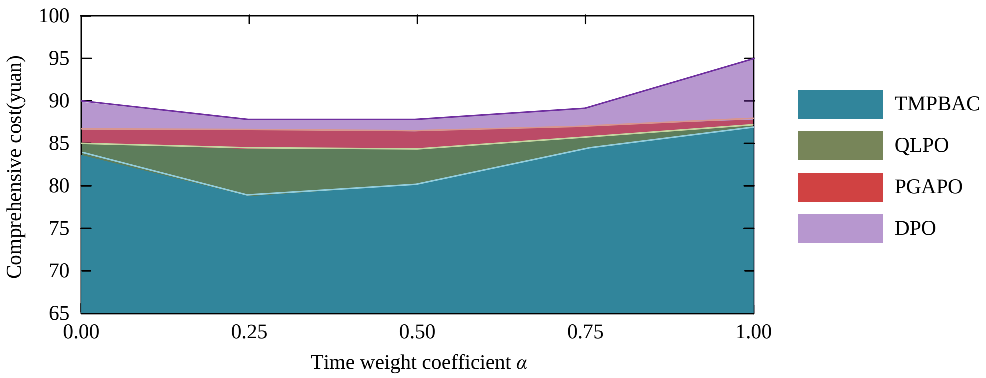

Figure 11: Comparison of four algorithms for fault recognition in three parts

computational efficiency of the optimal path. It can be promoted in practical travel path planning. In the analysis of the improvement effect of ATG preprocessing, when the traffic node reached 500, adding the ATG-ACO algorithm took only 43s, which was more than half of the time compared with the ant algorithm without ATG. The improved ATG improved the efficiency of ant algorithm in finding the optimal path. Feng et al. reached similar conclusions when conducting topology optimization on discrete structures in 2023 [19]. This result indicates that the improved topology has a clear and simplified structure, which can be used to design more efficient models for path planning. From the above results, the improved ATG algorithm can remove redundant paths. Combining with the ACO algorithm can not only improve iteration efficiency, but also avoid getting stuck in local optima and reduce computational cost, which other expensive algorithms do not have these effects. Finally, in the analysis of the comprehensive cost control effect of the ATG-ACO model, the results showed that when only considering a single cost of time or charging fees, the proposed model was not entirely superior to other models. However, considering both travel time and charging cost, the ATG-ACO model was completely superior to other models. Under different weighting coefficients, the average total cost of the research model was 7%-26% lower than other models. This result is similar to the research findings of Nadjib and Ammar in combining ATG and ACO algorithms [20]. From the above results, the research model introduces the conversion coefficient to convert the multi-objective problem into a single-objective problem, introduces the weighting coefficient to balance the weight of time and cost, and adopts PSO for optimization, so as to minimize the total cost. Other models do not have such powerful nonlinear programming capabilities, so the effect of the research model is better than other models. This result indicates that the travel path planning model based on the ATG-ACO algorithm meets the optimization requirements for travel paths that comprehensively consider travel time and charging cost. There is much research closely related to the path planning of electric vehicles. The intelligent algorithm greatly improves the superiority of path planning. However, the addition of conversion coefficient and weighting coefficient for different groups to balance the charging cost and travel time is a unique contribution of the research.

5 Conclusion

The study focused on how to comprehensively consider travel time and charging cost to plan paths during long-distance driving of electric vehicles. The improved ATG was combined with the ant path optimization algorithm. The combined method is used to calculate total travel cost. Then, a path optimization model was constructed. The research model introduced a topology graph to heterogeneous roads during travel, and improved the ATG. The ant algorithm was introduced into the preprocessed topology graph to form a new optimization algorithm for finding the optimal path. Combining the combination algorithm with the comprehensive total cost calculation method and iteratively finding the optimal path, an electric vehicle travel path optimization model considering balance time and charging cost was constructed. The study conducted simulation experiments. The simulation results showed that the improved ATG had a great promoting effect on ant algorithm path planning. The research model had a better balance effect than other models in considering the total travel time and total charging cost, and the comprehensive total cost of the optimal path was the lowest. Path planning is a particularly complex systemic problem, especially when long-distance travel is influenced by many factors. In addition to the electricity level and charging and discharging status mentioned in the article, there are other factors, including electric vehicle malfunctions, temporary traffic accidents, and congestion. Although the probability of an event occurring is extremely low, it can also have impacts on the travel path and total cost, which is also an area that needs improvement in the future.

References

[1] V. Boglou, A. Christos-Spyridon Karavas, Karlis, and K. Arvanitis, “An intelligent decentralized energy management strategy for the optimal electric vehicles' charging in low-voltage islanded microgrids,” International Journal of Energy Research, vol. 46, no. 3, pp. 2988-3016, 2022. https://doi.org/10.1002/er.7358

[2] D. P. Kumar, B. M. Younus, and S. Shambhu, “Life cycle assessment of electric vehicles: a systematic review of literature,” Environmental Science and Pollution Research, vol. 31, no. 1, 73-89, 2024. https://doi.org/10.1007/s11356-023-30999-3

[3] J. Nishanthy, S. C. Raja, T. Praveen, J. J. D. Nesamalar, and P. Venkatesh, “Techno-economic analysis of a hybrid solar wind electric vehicle charging station in highway roads,” International Journal of Energy Research, vol. 46, no. 6, pp. 7883-7903, 2022. https://doi.org/10.1002/er.7688

[4] T. Zhao, D. Cao, J. Yao, and S. Zhang, “Topology optimization algorithm for UAV formation based on wireless ultraviolet communication. Photonic Network Communications,” vol. 45, no. 1, pp. 25-36, 2023. https://doi.org/10.1007/s11107-022-00989-5

[5] Y. Li, C. Wang, W. Cao, D. and Hou, C. Zhang, “Motion characteristics simulations of supercavitating vehicle based on a three-dimensional cavity topology algorithm,” Applied Mathematical Modelling, vol. 115, no. 1, pp. 691-705, 2023. https://doi.org/10.1016/j.apm.2022.11.008

[6] L. Lucky, and A. S. Girsang, “Hybrid nearest neighbors ant colony optimization for clustering

social mMedia comments," Informatica, vol. 44, no. 1, pp. 63-74, 2020. https://doi.org/10.31449/inf.v44i1.2672

[7] L. Huo, "The global path planning for vehicular communication using ant colony algorithm in emerging wireless cloud computing," Wireless Networks, vol. 29, no. 2, pp. 833-842, 2023. https://doi.org/10.1007/s11276-022-03152-0

[8] H. Wang, "Research on data transmission optimization of communication network based on reliability analysis," Informatica, vol. 44, no. 3, pp. 361-366, 2020. https://doi.org/ https://doi.org/10.31449/INF.V44I3.3280

[9] D. Xia, B. Shen, Y. Zheng, W. Zhang, D. Bai, Y. Hu, and H. Li, "A bidirectional-a-star-based ant colony optimization algorithm for big-data-driven taxi route recommendation," Multimedia Tools and Applications, vol. 83, no. 6, pp. 16313-16335, 2024. https://doi.org/10.1007/s11042-023-15498-4

[10] Z. R. Dong, X. Y. Bian, and S. Zhao, "Ship pipe route design using improved multi-objective ant colony optimization," Ocean Engineering, vol. 258, no. 15, 1-14, 2022. https://doi.org/10.1016/j.oceaneng.2022.111789

[11] T. Zhao, A. A. Alshannaq, D. W. Scott, and G. H. Paulino, "Strut-and-tie models using multi-material and multi-volume topology optimization: load path approach," ACI Structural Journal, vol. 120, no. 6, pp. 7-22, 2023. https://doi.org/10.14359/51739089

[12] K. Li, and G. Cheng, "Structural topology optimization of elastoplastic continuum under shakedown theory," International Journal for Numerical Methods in Engineering, vol. 123, no. 19, pp. 4459-4482, 2022. https://doi.org/ 10.1002/nme.7041

[13] M. Montemurro, T. Roine, and J. Pailhes, "Multi-scale design of multi-material lattice structures through a CAD-compatible topology optimisation algorithm," Engineering Structures, vol. 273, no. 15, pp. 74-91, 2022. https://doi.org/10.1016/j.engstruct.2022.115009

[14] J. W. Han, S. Jeon, and H. J. Kwon, "Hierarchical Topology Map with Explicit Corridor for global path planning of mobile robots," Intelligent Service Robotics, vol. 16, no. 2, pp. 195-212, 2023. https://doi.org/ 10.1007/s11370-023-00458-6

[15] M. B. Sushma, S. Roy, and A. Maji, "Exploring and exploiting ant colony optimization algorithm for vertical highway alignment development," Computer-aided Civil and Infrastructure Engineering, vol. 37, no. 12, pp. 1582-1601, 2022. https://doi.org/10.1111/mice.12814

[16] H. Zheng, J. Guo, Q. Zhou, Y. Peng, and Y. Chen, "Application of improved ant colony algorithm in load balancing of software-defined networks," Journal of Supercomputing, vol. 79, no. 7, pp. 7438-7460, 2023. https://doi.org/10.1007/s11227-022-04957-8

[17] Z. Tang, H. Ma, "Path guidance method for unmanned vehicle based on improved potential field ant colony algorithm. International Journal of Vehicle Design," vol. 89, no. 1, pp. 84-97, 2022. https://doi.org/10.1504/ijvd.2022.10053059

[18] A. M. Abdullah, E. Ozen, H. Bayramoglu, "Energy efficient MANET routing protocol based on ant colony optimization," Ad Hoc & Sensor Wireless Networks, vol. 47, no. 1, pp. 73-96, 2020.

[19] F. Feng, S. Xiong, Z. Liu, Z. Xian, Y. Zhou, H. Kobayashi, A. Kawamoto, T. Nomura, and B. Zhu, "Cellular topology optimization on differentiable voronoi diagrams," International Journal for Numerical Methods in Engineering, vol. 124, no. 1, pp. 282-304, 2023. https://doi.org/10.1002/nme.7121

[20] N. Benaouda, A. Lahlouhi, "Ant-based delay-bounded and power-efficient data aggregation in wireless sensor networks," International Journal of Pervasive Computing and Communications, vol. 15, no. 2, pp. 97-119, 2019. https://doi.org/10.1108/IJPCC-04-2019-0037